Cooling of compact stars: effects of axions and dense QCD

Armen Sedrakian

Goethe-University, Frankfurt Main, Germany

"Phase of Dense Matter", INT, Seattle July 26, 2016

Cooling of compact stars

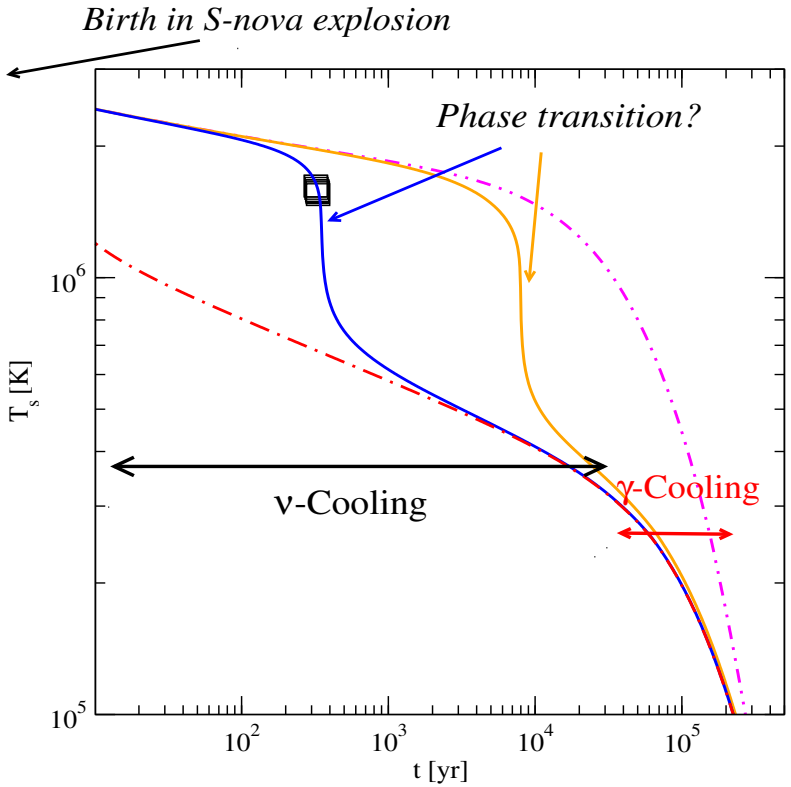

$$\left(\int_0^{R_c} nc_v(r,T)dV_p\right)\frac{dT'}{dt} = -\int_0^{R_c} n\epsilon_\nu(r,T)e^{2\Phi}dV_p + 4\pi\sigma R^2 T_S^4 e^{2\Phi_c}$$

Neutrino and photon radiation processes

- Modified Urca/brems process

$$n + n \to n + p + e + \bar{\nu},$$
$$n + n \to n + p + \nu + \bar{\nu},$$

- Crustal bremsstrahlung

$$e + (A, Z) \to e + (A, Z) + \nu + \bar{\nu},$$

- Cooper pair-breaking-formation

$$[NN] \to [NN] + \nu + \bar{\nu}.$$

- Surface photo-emission

$$L_\gamma = 4\pi\sigma R^2 T^4$$

- Quark Urca process

$$d \to u + e + \bar{\nu}, \quad u + e \to d + \nu.$$

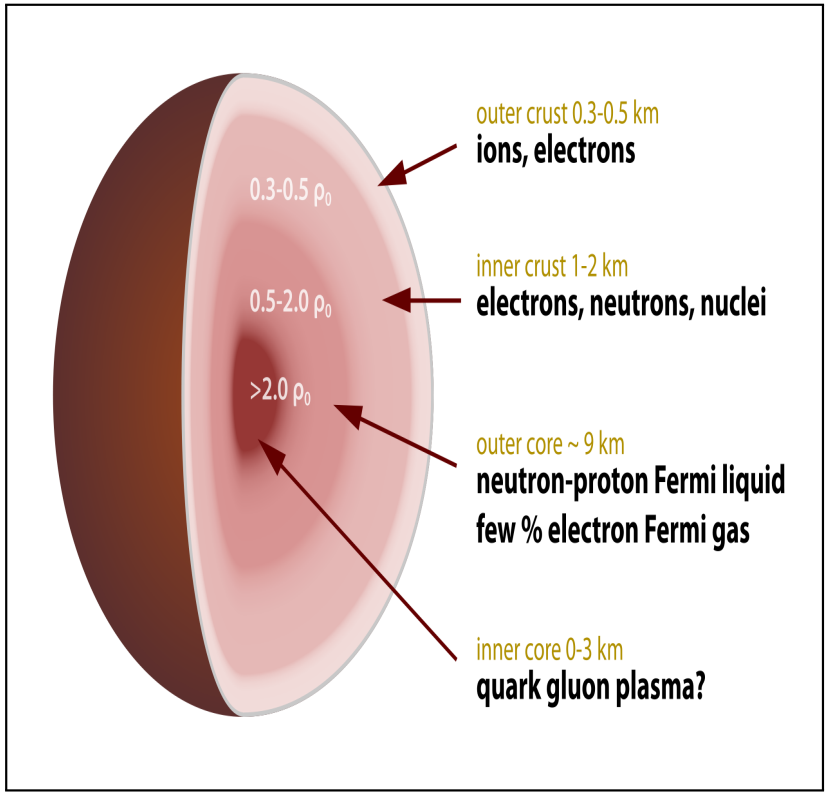

Strategies for NS constrains on axions

- Among the population of NS with measured surface temperature those that are warm are expected to have canonical masses $M \sim 1.4 M_{\odot}$. (No exotic process are operating in their interiors). Thus, the physics of cooling is dominated by well-constrained nuclear physics of NS.
- Use a benchmark code (NSCool, D. Page) with standard input (APR EOS and gaps) to make results easy to check. (Note that in QCD part we use our own code tailored to treat quark matter phases, see arXiv:1509.06986).
- One single data point is sufficient to put a tight constraint on axion properties via cooling. We keep only data that is considered reliable (Cas A + several NS with age 10^5 yr).
- Among the continuum of models define by the coupling constants choose the most conservative ones $C_e = 0$ (hadronic model of axions KVSZ).

- Most of the axion process relevant for NS cooling were computed by Iwamoto, Burrows 80'a, Raffelt et al., Reddy et al in 90's
- First cooling simulations with axions in conference proceedings by Umeda, Tsuruta, Iwamoto in 1998 and then complete silence until 2015 [arXiv:astro-ph/9806337]
- Pair-breaking processes - J. Keller and A. S. (NPA, 2013) [arXiv:1205.6940]
- Full scale cooling simulations - A. S. (PRD, 2016) [arXiv:1512.07828]

Recent progress on emissivities

The neutrino emissivity is expressed in terms of the polarization tensor of baryonic matter

$$\varepsilon_{\nu\bar{\nu}} = -2\left(\frac{G_F}{2\sqrt{2}}\right)^2 \int d^4q g(\omega)\omega \sum_{i=1,2} \int \frac{d^3q_i}{(2\pi)^3 2\omega_i} \mathrm{Im}[L^{\mu\lambda}(q_i)\,\Pi_{\mu\lambda}(q)]\delta^{(4)}(q - \sum_i q_i),$$

Four polarization tensors in Nambu-Gorkov space:

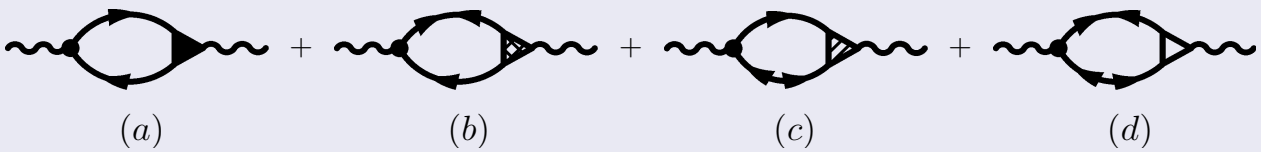

Effective Bethe-Salpeter equations for vertices:

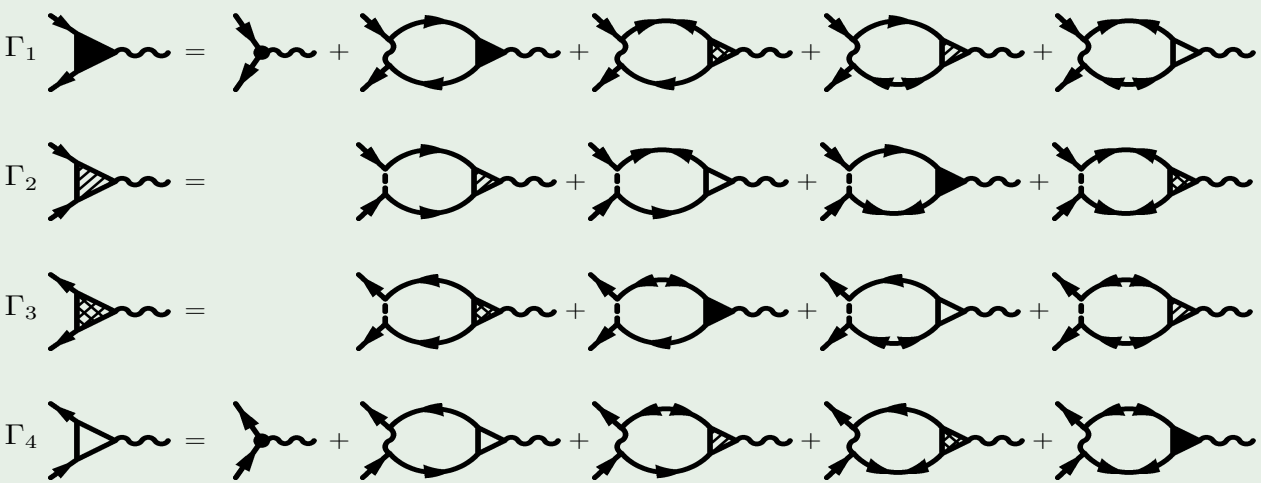

Vector current emissivity

The vector current emissivity is given by

$$\epsilon = \frac{16 G^2 c_V^2 \nu(0) v_F^4}{1215\pi^3} I(z) T^7,$$

$$I(z) = z^7 \int_1^\infty \frac{dy\, y^5}{\sqrt{y^2-1}} f\,(zy)^2 \times \left[1 + \left(\frac{7}{33} + \frac{41}{77}\gamma\right) v_F^2\right].$$

$z \equiv \Delta/T$.

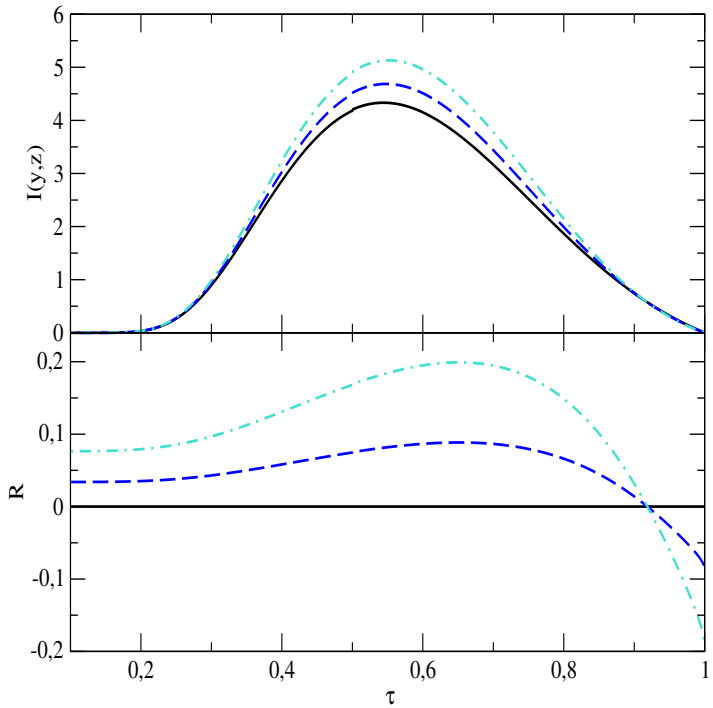

- Systematic expansion in v_F^2, leading order at v_F^4
- The next-to-leading correction in v_F^2 which is $O(v_F^6)$ contributes about 10%.
- The emissivity has a maximum at $\tau = T/T_c = 0.6$, i.e., affects cooling close to the phase transition

Results due to Leinson-Perez (2006) Kolomeitsev-Voskresensky (2008) Reddy-Steiner (2008) A. S. et al (2007,2012)

Axial current emissivity

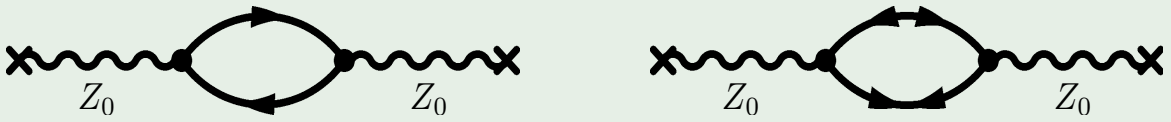

The two diagrams contributing to the polarization tensor of baryonic matter, which defines the axial vector emissivity. The "normal" baryon propagators for particles (holes) are shown by single-arrowed lines directed from left to right (right to left). The double arrowed lines correspond to the "anomalous" propagators F (two incoming arrows) and F^+ (two outgoing arrows).
The emissivity of this processes is given by

$$\epsilon_\nu = \frac{4G_F^2 g_A^2}{15\pi^3}\zeta_A \nu(0) v_F{}^2 T^7 I_\nu, \quad I_\nu = z^7 \int_1^\infty dy \frac{y^5}{\sqrt{y^2-1}} f_F\,(zy)^2\,. \tag{1}$$

Note the v_F^2 scaling of the axial neutrino emissivity compared to the v_F^4 scaling.

Axial neutrino emissivity dominates the vector current emissivity because of v^2 scaling instead of v^4 scaling.

The strong CP problem

The origin of axions

$$\mathcal{L}_{QCD} = \sum_q \bar{\psi}_q (iD - m_q e^{i\theta_q})\psi_q - \frac{1}{4} G_{\mu\nu a} G_a^{\mu\nu} - \theta \frac{\alpha_s}{8\pi} G_{\mu\nu a} \tilde{G}_a^{\mu\nu} \tag{2}$$

The phase can be pushed in the last term by chiral rotation $\psi_q' = e^{-i\gamma_5 \theta_q/2}\psi_q$

$$\mathcal{L}_{QCD} = \sum_q \bar{\psi}_q (iD - m_q)\psi_q - \frac{1}{4} G_{\mu\nu a} G_a^{\mu\nu} - \underbrace{(\theta - \arg\det M_q)}_{\bar{\theta}} \frac{\alpha_s}{8\pi} G_{\mu\nu a} \tilde{G}_a^{\mu\nu} \tag{3}$$

Experimental value: $\bar{\theta} \leq 10^{-11}$ comes from neutron electric dipole moment

$$|d| = 0.63 \times 10^{-25}\, e\, cm \tag{4}$$

The strong CP problem - smallness of $\bar{\theta}$ (unnatural). Reinterpretation of $\bar{\theta}$ term as a dynamical field pseudo-scalar axion field $a(x)$ with decay constant f_a

$$\mathcal{L}_{CP} = -\frac{\alpha_S}{8\pi} \bar{\theta} \mathrm{Tr} G\tilde{G} \quad \rightarrow \quad \mathcal{L}_{CP} = -\frac{\alpha_S}{8\pi} \frac{a(x)}{f_a} \mathrm{Tr} G\tilde{G} \tag{5}$$

The potential (mass term) forces the field to its minimum where $\bar{\theta} = 0$.

Global constraints on axion mass

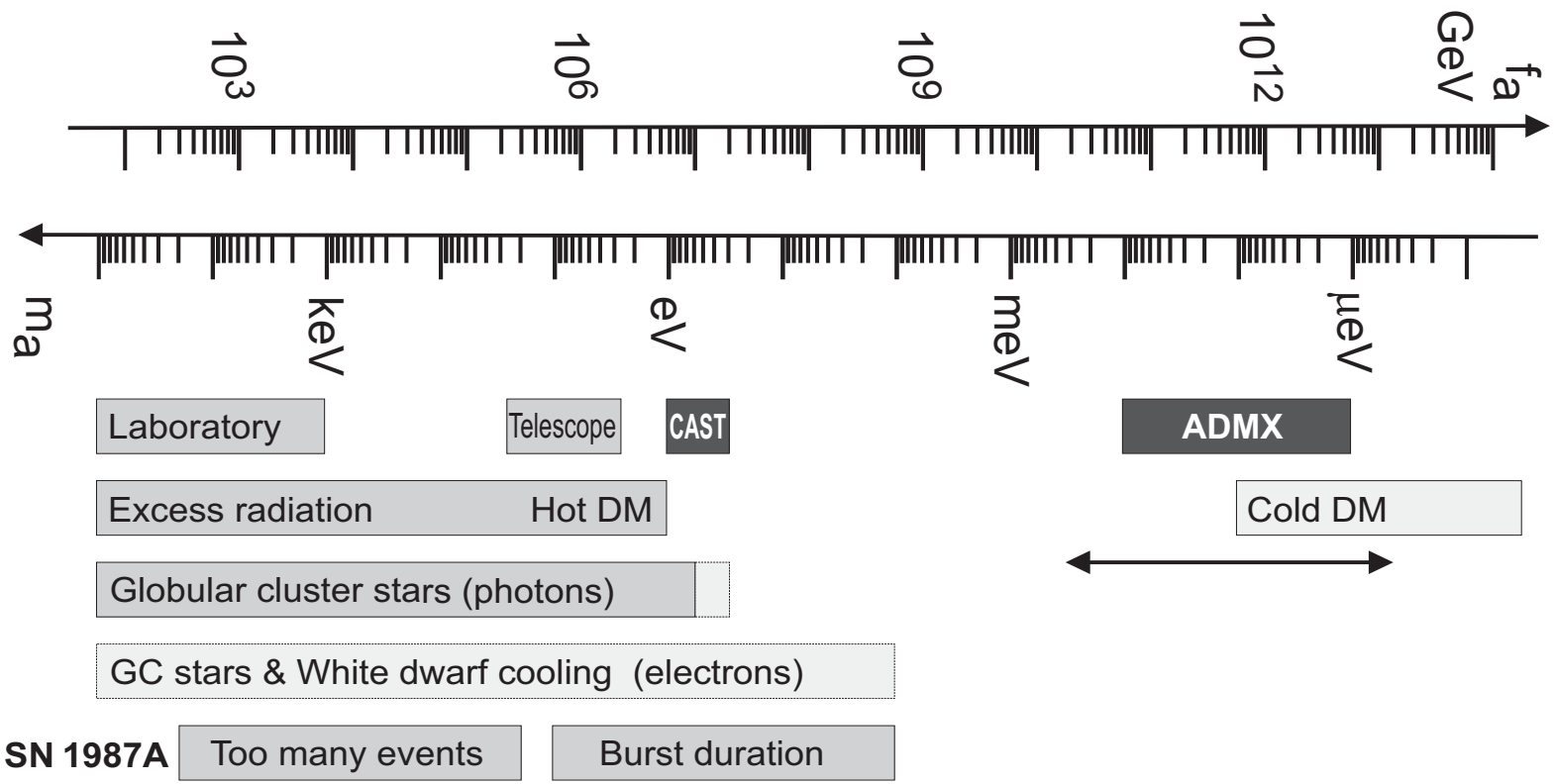

Axion emissivity

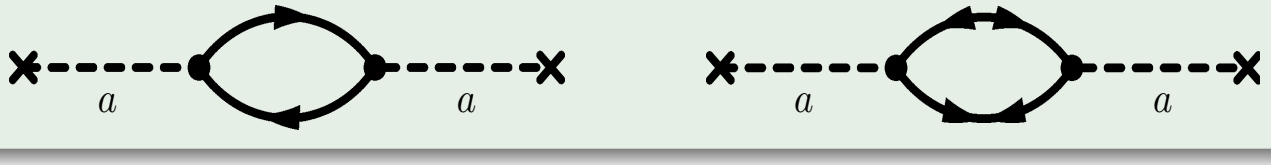

Key diagrams contributing to the axion pair-breaking emissivities are at one-loop level.

Axion emissivity for S-wave condensate

$$\epsilon^S_{aN} = \frac{2C_N^2}{3\pi} f_a^{-2}\, \nu_N(0)\, v_{FN}^2\, T^5\, I^S_{aN},$$

$$I^S_{aN} = z_N^5 \int_1^\infty dy\, \frac{y^3}{\sqrt{y^2-1}} f_F\,(z_N y)^2\,.$$

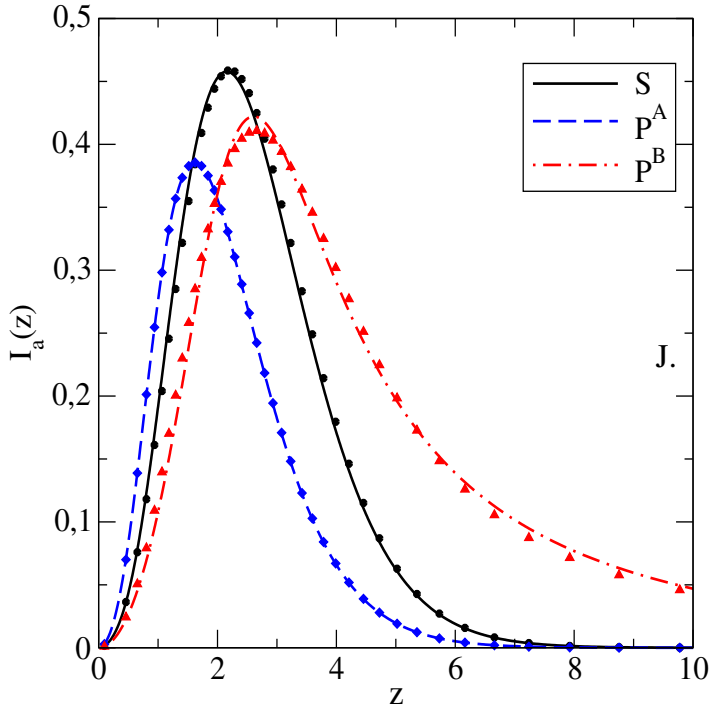

Keller and A. S. (NPA, 2013) [arXiv:1205.6940] for S-wave condensate, A. S. (PRD, 2016) [arXiv:1512.07828] for P-wave condensates

The C_N charges are generally given by generalized Goldberger-Treiman relations

$$C_p = (C_u - \eta)\Delta_u + (C_d - \eta z)\Delta_d + (C_s - \eta w)\Delta_s, \quad (6)$$
$$C_n = (C_u - \eta)\Delta_d + (C_d - \eta z)\Delta_u + (C_s - \eta w)\Delta_s, \quad (7)$$

where $\eta = (1 + z + w)^{-1}$, with $z = m_u/m_d$, $w = m_u/m_s$, and $\Delta_u = 0.84 \pm 0.02$, $\Delta_d = -0.43 \pm 0.02$ and $\Delta_s = -0.09 \pm 0.02$, $z = m_u/m_d = 0.35$–0.6.

For *hadronic axions*, $C_{u,d,s} = 0$, and the nucleonic charges vary in the range

$$\boxed{-0.51 \leq C_p \leq -0.36, \quad -0.05 \leq C_n \leq 0.1.} \quad (8)$$

- neutrons may not couple to axions ($C_n = 0$)
- protons always couple to axions $C_p \neq 0$
- invisible axion DFSZ model

$$C_e = \cos^2\beta/3, \quad C_u = \sin^2\beta/3, \quad C_d = \cos^2\beta/3, \quad \text{arbitrary } \beta$$

- KVSZ model $C_e = 0$ and C_p and C_n from above inequalities

The axion mass is related to f_a via the relation

$$m_a = \frac{z^{1/2}}{1+z}\frac{f_\pi m_\pi}{f_a} = \frac{0.6\,\text{eV}}{f_a/10^7\ \text{GeV}} \quad m_\pi = 135\,\text{MeV},\ f_\pi = 92\ \text{MeV},\ z = 0.56. \quad (9)$$

Constraining axion parameters

We now require that the axion luminosity does not exceed the neutrino luminosity

$$\frac{\epsilon_a}{\epsilon_\nu} = \frac{\alpha}{f_a^2 G_F^2 \Delta(T)^2} < 1, \tag{10}$$

where we set the ratio $I_a/I_\nu \simeq 1$ and find that $\alpha \simeq 73.7$ ($g_A = 1.25$). Our bound is given by (J. Keller quand A. Sedrakian, Nucl. Phys. A, 897, 62, 2013)

$$\boxed{f_a > 7.4 \times 10^9 \text{ GeV} \left[\frac{0.1 \text{ MeV}}{\Delta(T)}\right],} \tag{11}$$

which translates into an upper bound on the axion mass

$$m_a = 0.62 \times 10^{-3} \text{ eV} \left(\frac{10^{10}\text{GeV}}{f_a}\right) \leq 0.84 \times 10^{-3} \text{ eV} \left[\frac{\Delta(T)}{0.1 \text{ MeV}}\right]. \tag{12}$$

The bound on f_a can be written in terms of the critical temperature by noting that $\Delta(T) \simeq 3.06 T_c \sqrt{1 - T/T_c} \simeq T_c$ in the temperature range $0.5 \leq T/T_c < 1$ of most interest.

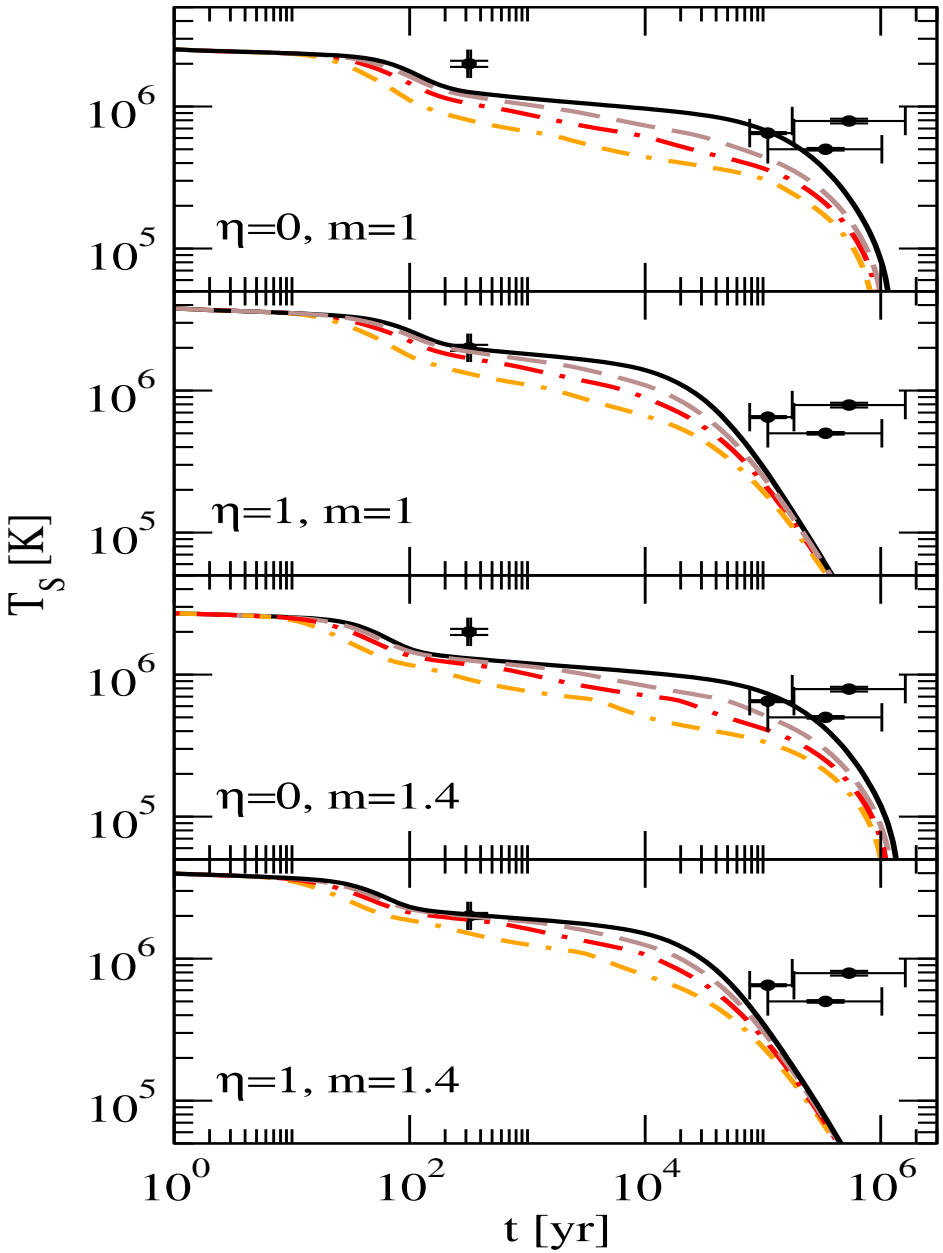

Figure : the case $f_{a7} = \infty$ (solid line) 10 (dashed), 5 (dash-dotted), and 2 (double-dash-dotted).

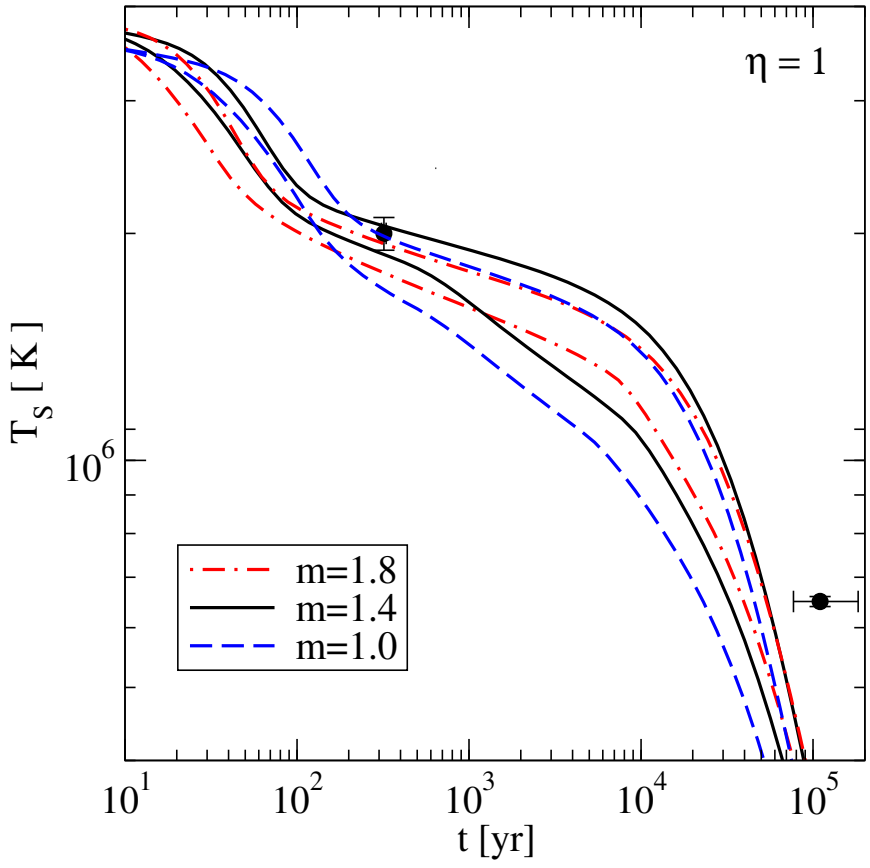

Figure : Cooling tracks of neutron star models with masses $m = 1$ (dash-dotted) 1.4 (solid) and 1.8 (dashed) for the case of an accreted light-element envelope ($\eta = 1$) along with the measured temperature of CCO in Cas A. For each value of mass, the upper curve corresponds to the cooling without axions, and the lower curve corresponds to axion cooling with $f_{a7} = 5$. Note the weak dependence on the surface temperature of models on the star mass.

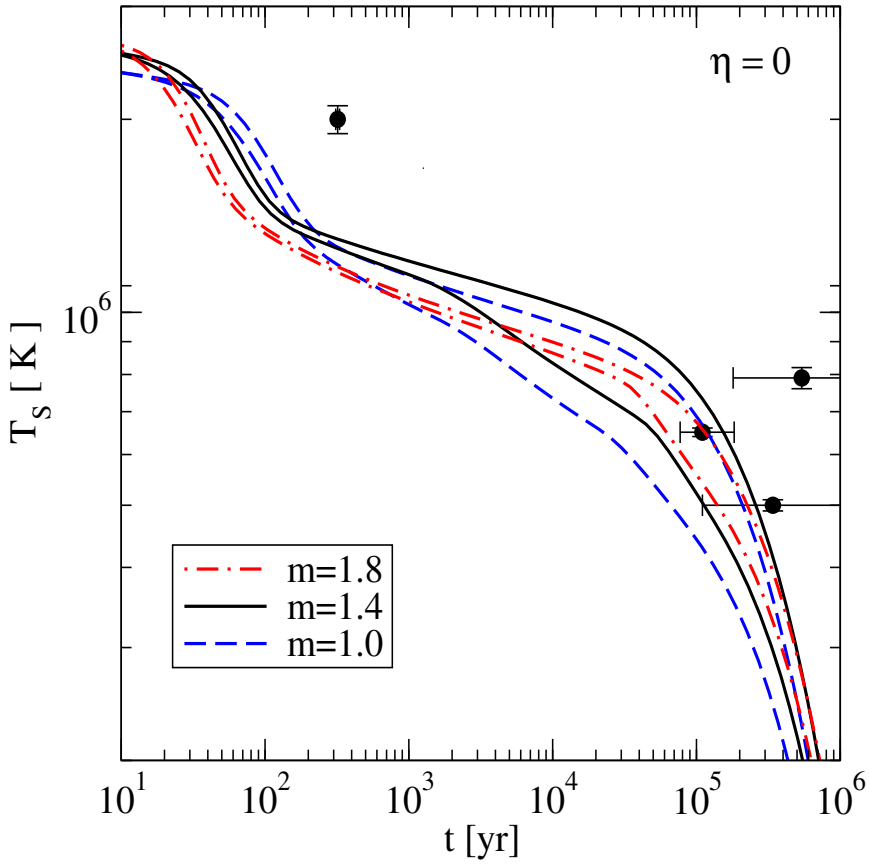

Figure : Cooling tracks of neutron star models with masses $m = 1$ (dashed) 1.4 (solid), and 1.8 (dash-dotted) for the case of a nonaccreted iron envelope ($\eta = 0$). The measured temperatures of PSR B0656+14, Geminga are consistent with neutrino cooling tracks; the uncertainty in the spin-down age of PSR B1055-52 and internal heating may account for marginal inconsistency. The axion cooling tracks are shown for $f_{a7} = 10$.

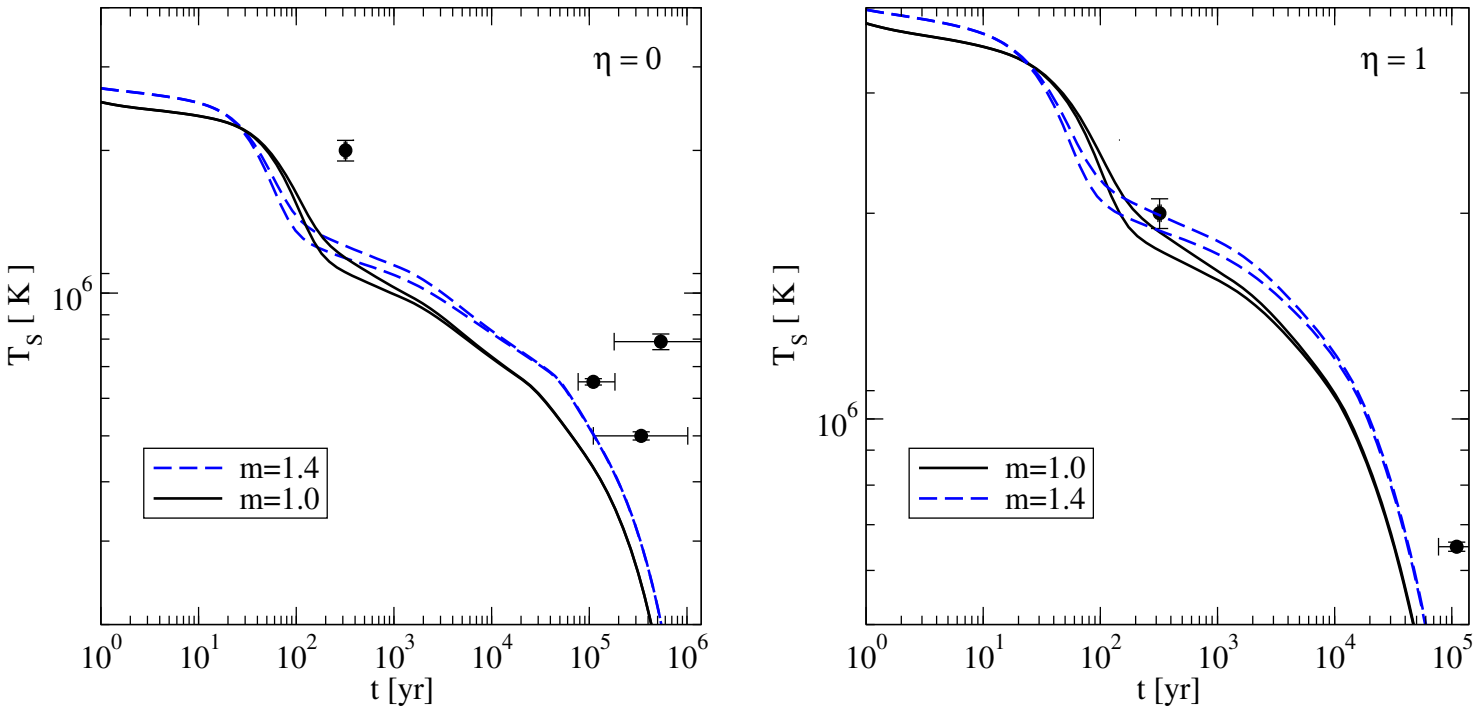

Figure : Cooling tracks of neutron star models with masses $m = 1$ (solid) and 1.4 (dashed) for the case of a nonaccreted iron envelope ($\eta = 0$) and accreted envelope ($\eta = 1$) and for $f_{a7} = 10$. For each mass, the two tracks differ by the value of the neutron PQ charge. The upper curves correspond to our standard choice $|C_n| = 0.04$, while the lower curves correspond to the case of enhanced axion emission with $|C_n| = |C_p| = 0.4$.

Updated global constraints on axion mass

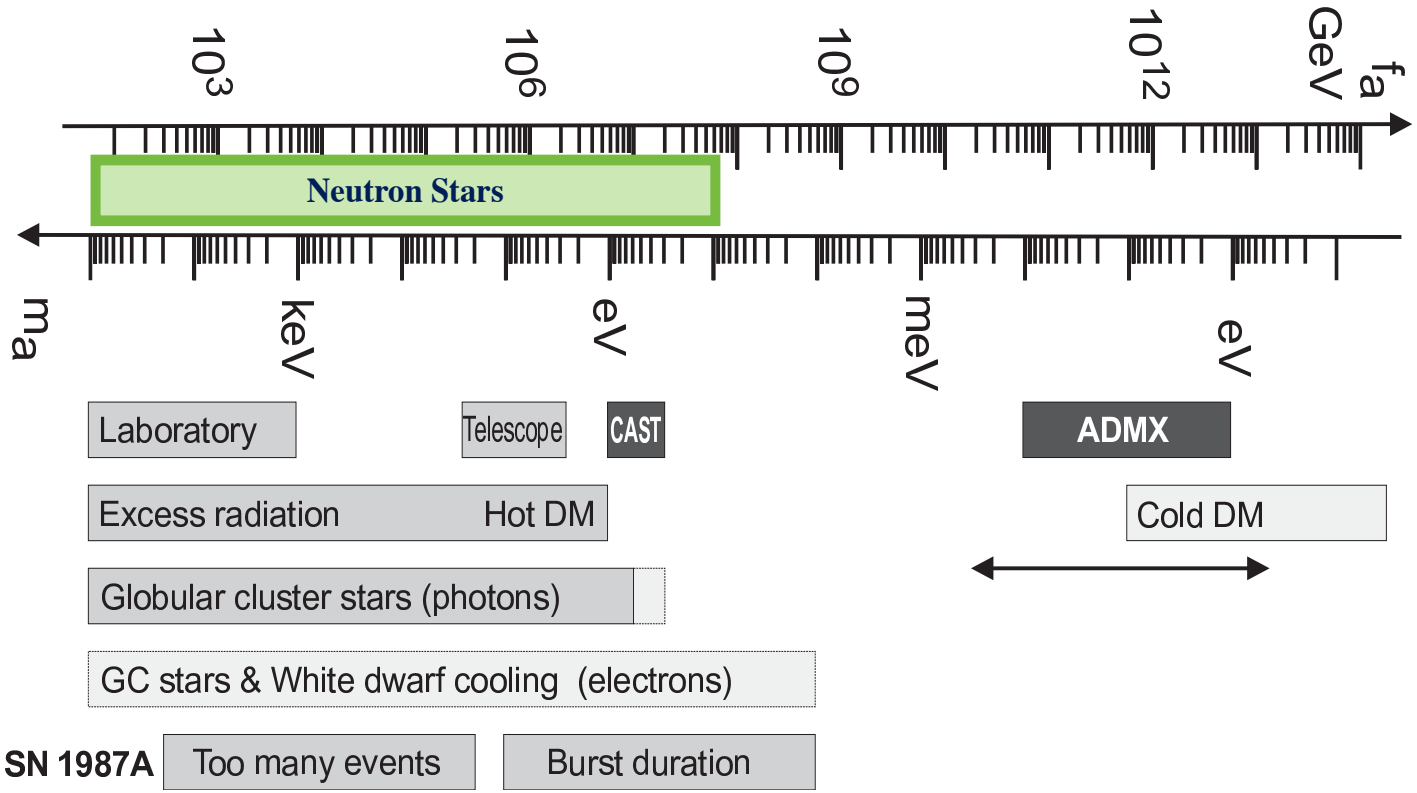

The NS constraint are based on highly conservative physics of hadronic matter and on benchmarked code for cooling simulations of NS.

Cas A remnant, cooling in course

Image shows Cassiopeia A the youngest supernova remnant in the Milky Way.

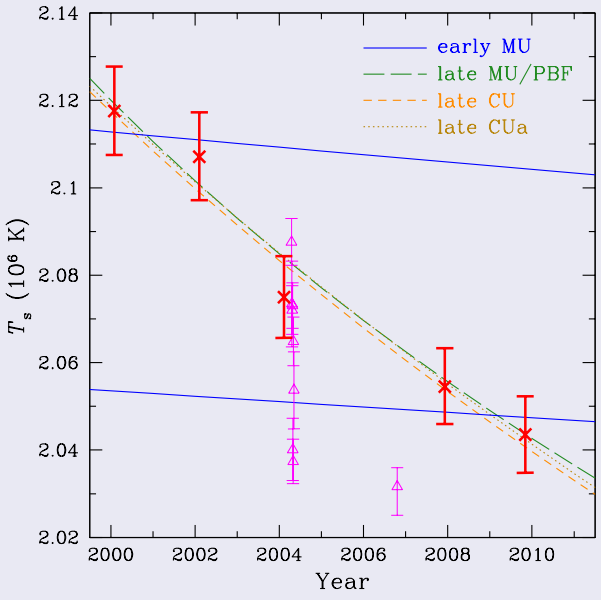

NASA's Chandra X-ray Observatory has discovered the first direct evidence for a superfluid. (Conclusions drawn from cooling simulations of the neutron stars).

Cas A remnant, cooling in course

Thermal history of Compact Stars

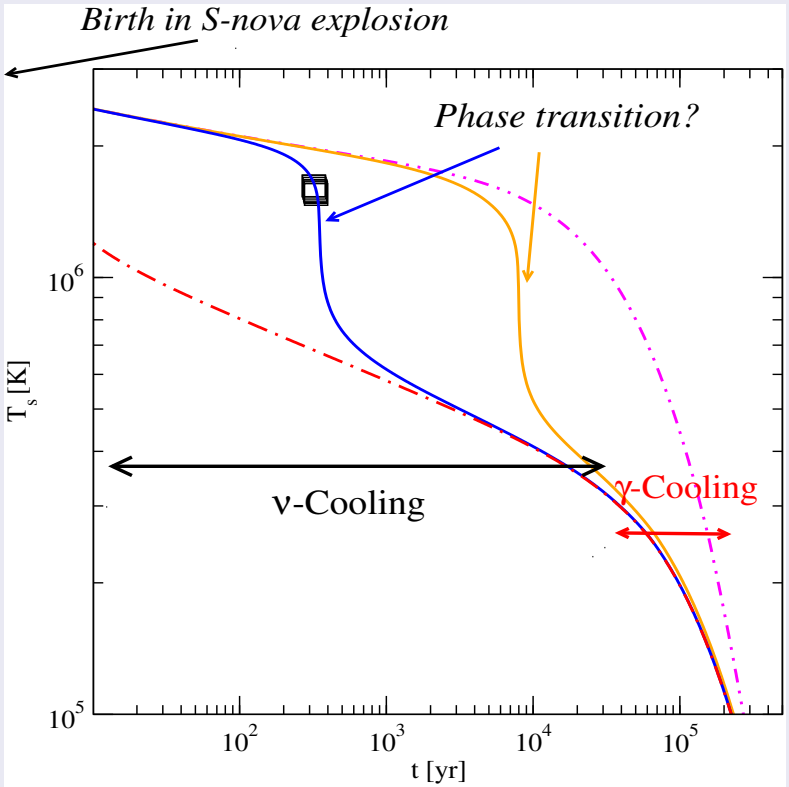

$$\boxed{\frac{\partial S}{\partial t} + \vec{\nabla} \cdot \vec{q} = \mathcal{R} - \mathcal{L}_\nu - \mathcal{L}_\gamma} \qquad dS = c_V dT, \quad \vec{q} = \kappa \vec{\nabla} T$$

- Dissipative function $\mathcal{R} \propto \sigma(\nabla\phi)^2 + \kappa(\nabla T)^2/T + \ldots$
- Neutrino losses $\mathcal{L}_\nu$ from the bulk
- Photon losses $\mathcal{L}_\gamma$ from the surface

Cooling processes in quark matter

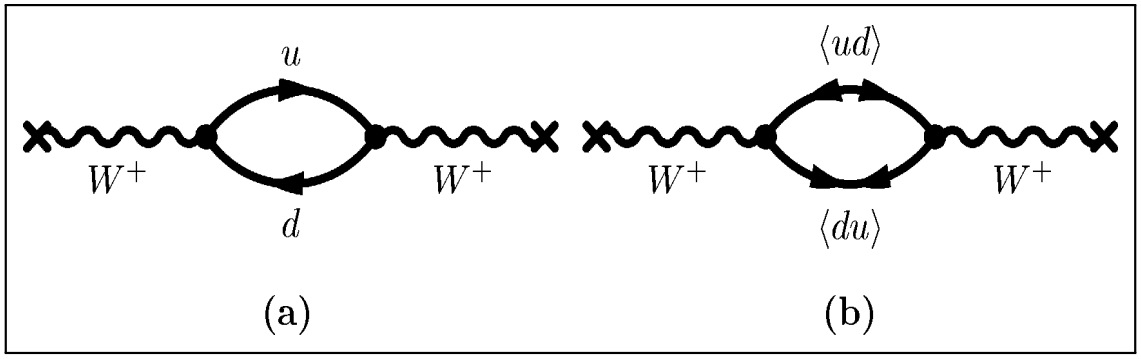

Feynman diagrams contributing to the Urca process $d \to u + e + \bar{\nu}_e$ and $u + e \to d + \nu_e$.

$$\epsilon_{\nu\bar{\nu}} \sim \sum_{\text{phase space}} \text{Im}\left[\Lambda^{\mu\lambda}(q_1, q_2)\, \Pi^R_{\mu\lambda}(q)\right].$$

where response function

$$\Pi_{\mu\lambda}(q) = -i \int \frac{d^4p}{(2\pi)^4} \text{Tr}\left[(\Gamma_-)_\mu S(p)(\Gamma_+)_\lambda S(p+q)\right], \quad \Gamma_\pm(q) = \gamma_\mu(1-\gamma_5) \otimes \tau_\pm$$

with propagators

$$S_{f=u,d} = i\delta_{ab} \frac{\Lambda^+(p)}{p_0^2 - \epsilon_p^2}(\not{p} - \mu_f\gamma_0), \quad F(p) = -i\epsilon_{ab3}\epsilon_{fg}\Delta \frac{\Lambda^+(p)}{p_0^2 - \epsilon_p^2}\gamma_5 C.$$

In the red-green color sector

$$\boxed{\zeta = \Delta_{rd}/\delta\mu, \qquad \delta\mu = (\mu_d - \mu_u)/2}$$

and in the blue color sector

$$\boxed{\Delta_b = 0 \qquad \Delta_b \neq 0.}$$

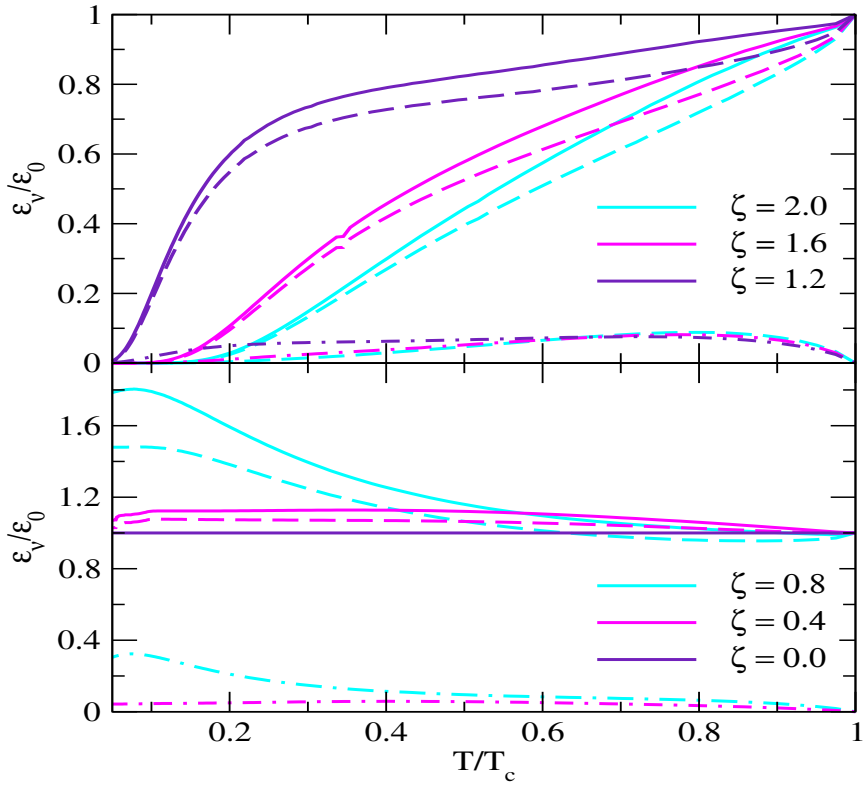

Figure : Upper panel: perfect 2SC phase $\zeta > 1$, Lower panel: crystalline phase $\zeta < 1$

Fix zeta simulations

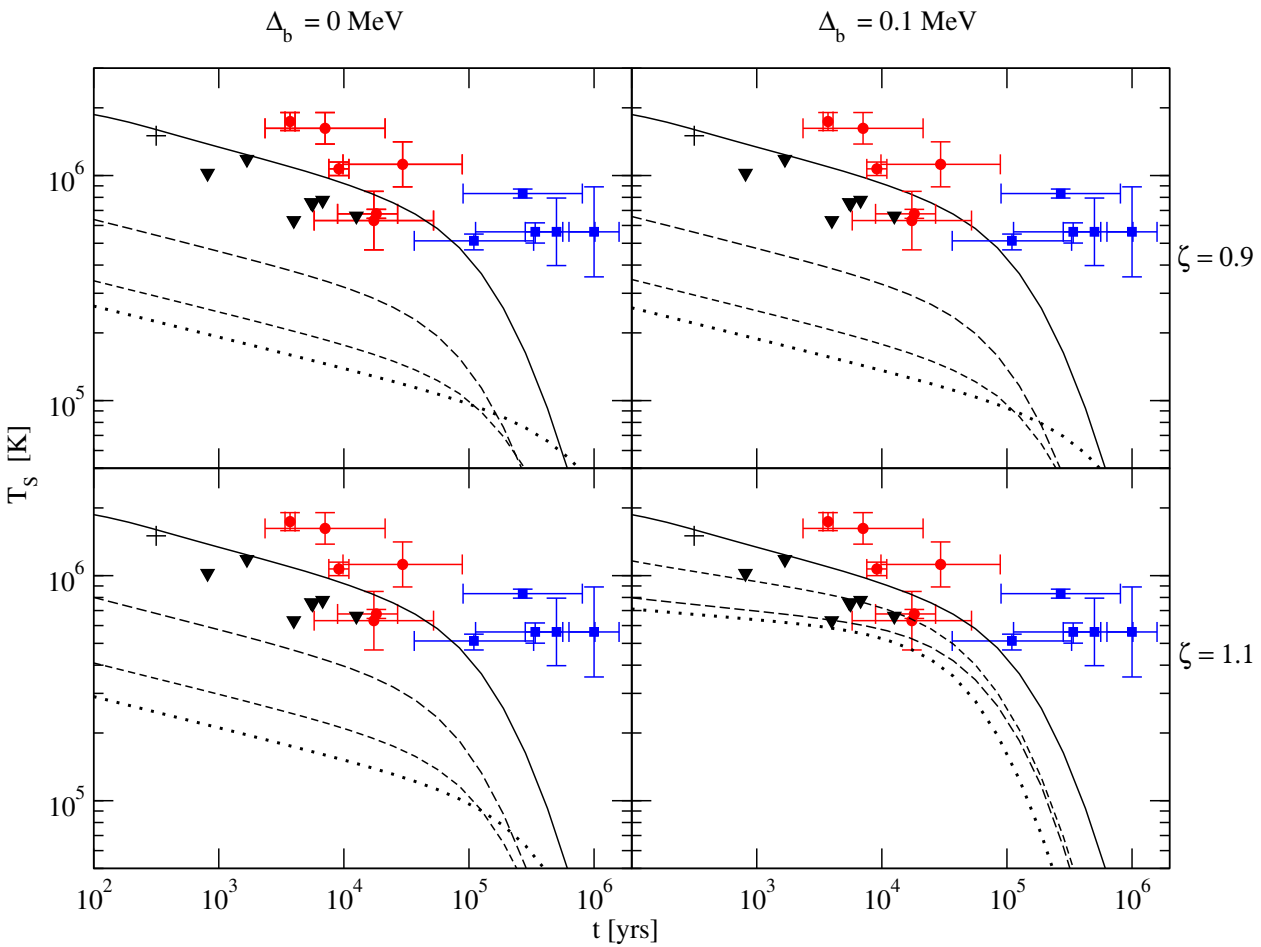

Two parameters in the theory are held fixed with cases

$$(a)\ \Delta_b = 0 \quad \zeta < 1 \quad (b)\ \Delta_b \neq 0 \quad \zeta < 1$$
$$(c)\ \Delta_b = 0 \quad \zeta > 1 \quad (d)\ \Delta_b \neq 0 \quad \zeta > 1$$

Phase transition within the QCD phase diagram can take place from one pairing pattern to the other (e.g. 2SC to Crystalline)

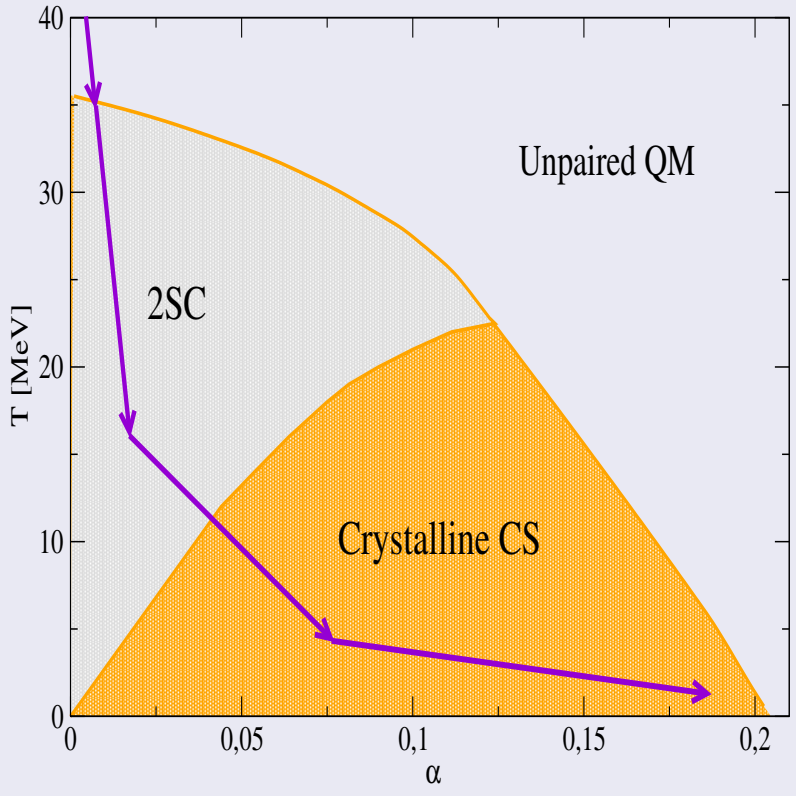

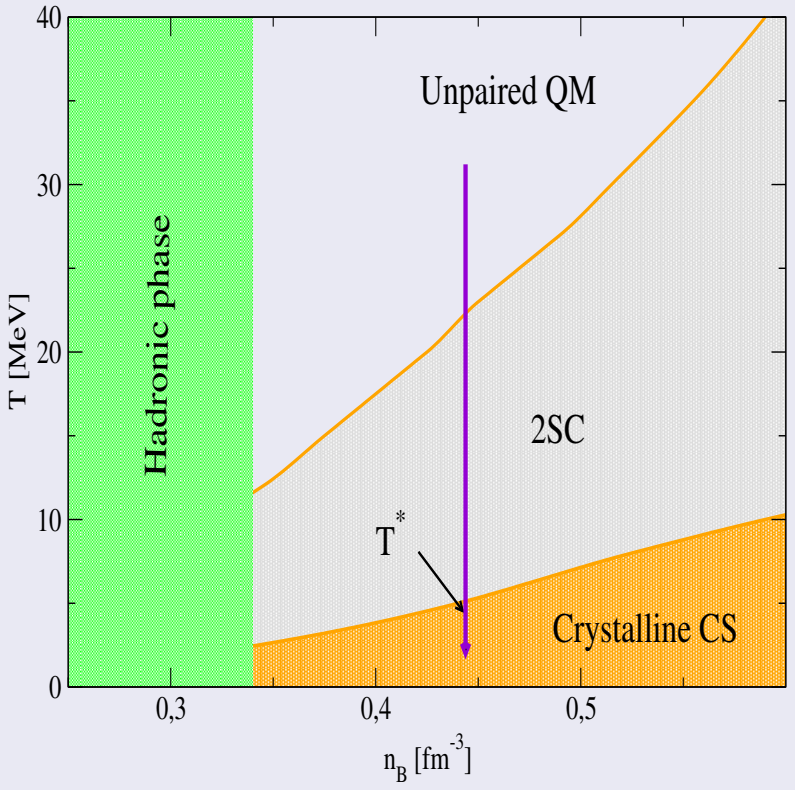

Left: Generic phase diagram of imbalanced fermi-systems; Right: β-equilibrated stellar matter

Parameters in the problem

- The critical phase transition temperature T^* to the CS phase
- The width (or duration of the transition)
- Properties (gap) in the blue condensate spectrum

Cas cooling as a phase transition in QCD

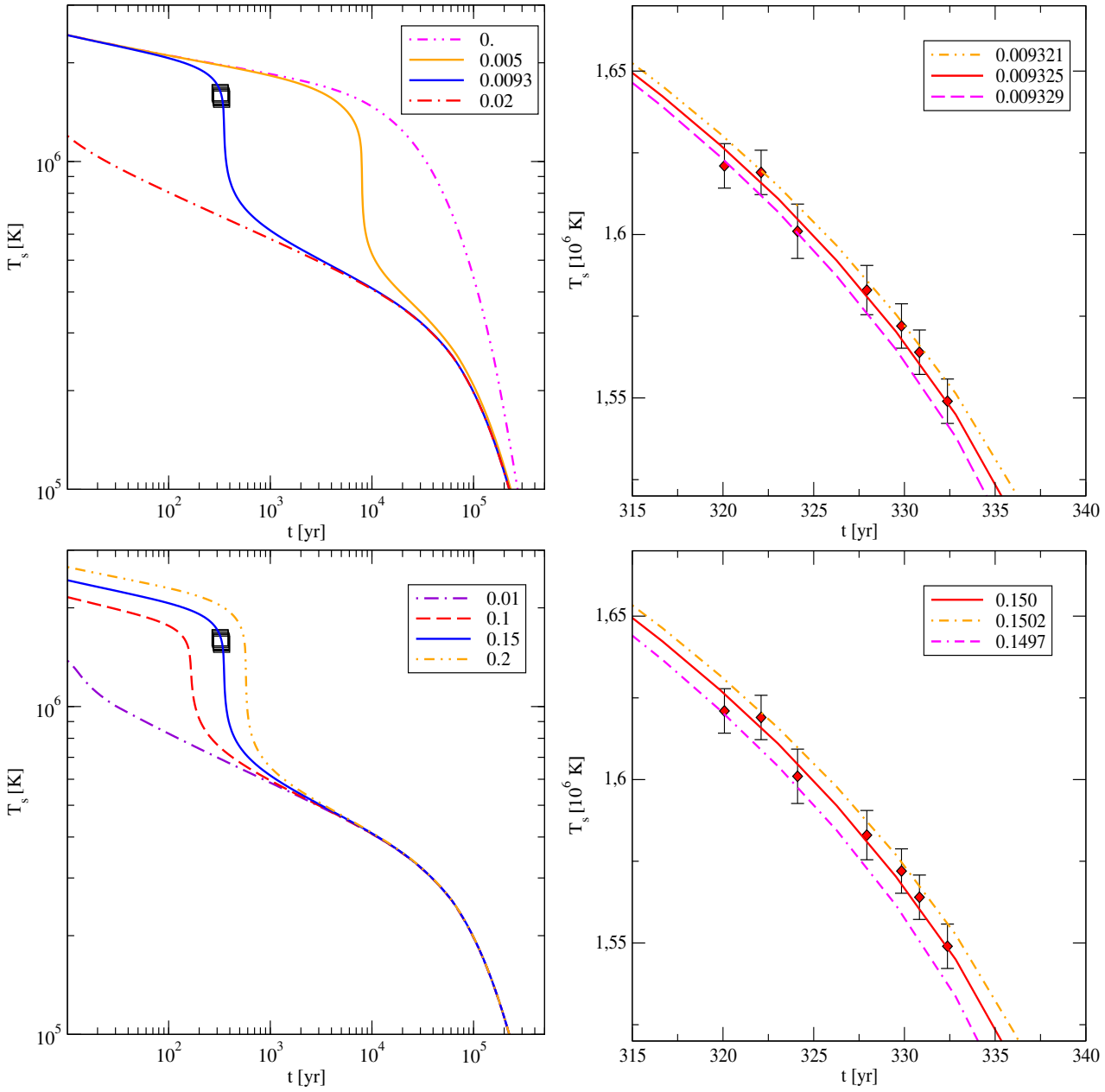

Summary

Summary

- NS cooling provides solid, conservative constraints on the axion properties
- Benchmark cooling simulations are comparable with other best astrophysical constrains (especially for the models of hadronic axions).
- Cooling simulations indicate that Cas A behaviour can be understood as a phase transition in QCD phase diagram
- This comes, of course, with all the uncertainties of our current understanding of non-perturbative QCD - best phenomenology we can do in the year to come